Impact on *r* of foreground B-modes : LiteBIRD forecasts with COMMANDER

Mathieu Remazeilles

MANCHESTER 1824
The University of Manchester

Remazeilles, Dickinson, Eriksen, Wehus
arXiv:1509.04714

B mode from space - IPMU Tokyo
10-16 Dec 2015

CMB B-mode polarization satellite concepts

Concept name	Leading country/ institution	Frequencies [GHz]	Beam size FWHM [arcmin]	Sensitivities [μK deg]	Reference/notes
EPIC-LC-TES	U.S.A. (NASA)	30,40,60,90 135,200,300	155,116,77,52, 34,23,16	0.460,0.156,0.085,0.037, 0.035,0.037,0.062	EPIC Low-Cost option with TES detectors (Bock et al. 2008)
EPIC-CS	U.S.A. (NASA)	30,45,70,100, 150,220,340,500	15.5,10.3,6.6,4.6, 3.1,2.1,1.4,0.9	0.683,0.367,0.150,0.117 0.117,0.183,0.883,7.50	EPIC Comprehensive-Science option (Bock et al. 2008)
EPIC-IM-4K	U.S.A. (NASA)	30,45,70,100,150 220,340,500,850	28,19,12,8.4,5.6 3.8,2.5,1.7,1.0	0.147,0.061,0.027,0.018,0.014, 0.027,0.058,0.014,0.012	EPIC Intermediate with 4 K mirror (Bock et al. 2009)
LiteBIRD	Japan (JAXA)	60,78,100, 140,195,280	75,58,45, 32,24,16	0.172,0.108,0.078, 0.062,0.0517,0.063	(Matsumura et al. 2013)
COrE	Europe (ESA)	45,75,105,135,165, 195,225,255,285,315, 375,435,555,675,795	23.3,14,10,7.8,6.4, 5.4,4.7,4.1,3.7,3.3, 2.8,2.4,1.9,1.6,1.3	0.150,0.078,0.077,0.075,0.077 0.075,0.075,0.173,0.283,0.767, 1.95,4.25,9.82,57.0,348.0	ESA M mission concept (The COrE Collaboration et al. 2011)
COrE+ Light	Europe (ESA)	60,70,80,90,100, 115,130,145,160,175, 195,220,255,295,340, 390,450,520,600	21.0,18.0,15.8,14.0,12.6, 11.0,9.7,8.7,7.9,7.2, 6.5,5.7,5.0,4.3,3.7, 3.2,2.8,2.4,2.1	0.485,0.467,0.320,0.257,0.197, 0.138,0.110,0.092,0.092,0.090, 0.090,0.135,0.218,0.430,0.817, 1.645,4.205,10.535,15.848	ESA M mission concept 3[1]
COrE+ Extended	Europe (ESA)	60,70,80,90,100, 115,130,145,160,175, 195,220,255,295,340, 390,450,520,600,700,800	14.0,12.0,10.5,9.3,8.4, 7.3,6.5,5.8,5.3,4.8, 4.3,3.8,3.3,2.9,2.5, 2.2,1.9,1.6,1.4,1.2, 1.1	0.342,0.233,0.160,0.123,0.098, 0.073,0.057,0.057,0.057,0.058, 0.063,0.090,0.152,0.220,0.422, 0.790,1.982,5.632,20.05,93.5,203	ESA M mission concept 4[1]
PRISM	Europe (ESA)	30,36,43,51,62, 75,90,105,135,160, 185,200,220,265,300, 320,395,460,555,660	17,14,12,10,8.2, 6.8,5.7,4.8,3.8,3.2 2.8,2.5,2.3,1.9,1.7, 1.6,1.3,1.1,0.92,0.77	0.211,0.141,0.133,0.103,0.098, 0.093,0.078,0.068,0.061,0.0572 0.059,0.061,0.064,0.073,0.085, 0.092,0.135,0.197,0.404,0.953	ESA L mission concept (André et al. 2014)
PIXIE	U.S.A. (NASA)	30,60,90,120,150, 180,210,240,270,300, 330,360,390,420,450, 480,510,540,570,600, 630,660,690,720,750, 780,810,840,870,900, 930,960,990,1020,1050, 1080,1110,1140,1170,1200	96.0 (constant)	5.180,1.390,0.691,0.454,0.352, 0.307,0.292,0.297,0.319,0.358 0.418,0.503,0.623,0.790,1.020, 1.350,1.800,2.440,3.350,4.660, 6.550,9.280,13.30,19.10,27.70, 40.50,59.60,88.20,131.00,196.00, 294.00,444.00,672.00,1020,1560, 2390,3670,5660,8750,13600	(Kogut et al. 2011)

No foreground : overall sensitivity

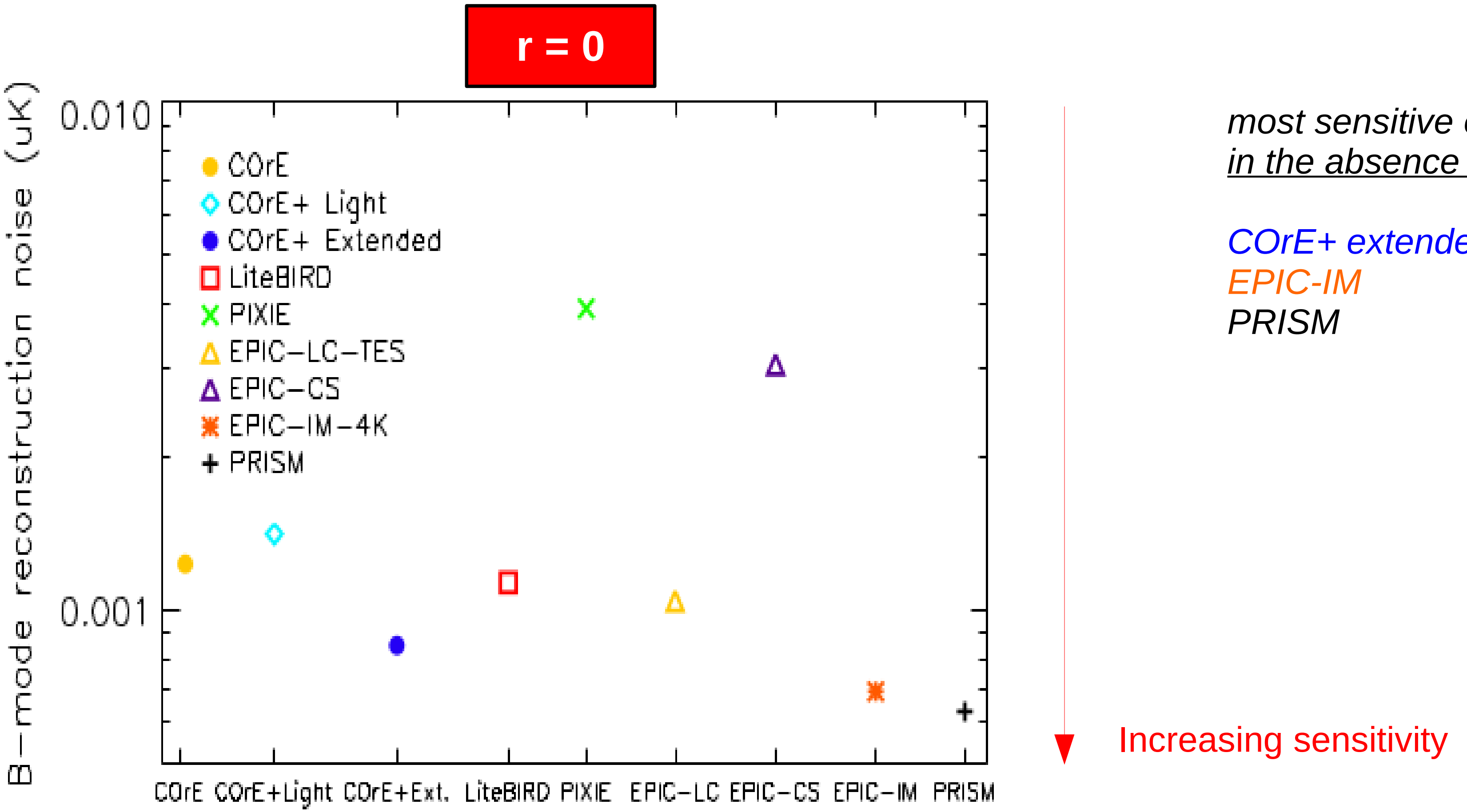

most sensitive experiments
<u>in the absence of foregrounds</u>:

COrE+ extended
EPIC-IM
PRISM

$\sim 1 / \sigma_{eff}^2 = \sum_i 1 / \sigma_i^2$ inverse variance weighting across frequencies

Remazeilles, Dickinson, Eriksen, Wehus, *arXiv:1509.04714*

CMB versus Foreground B-modes

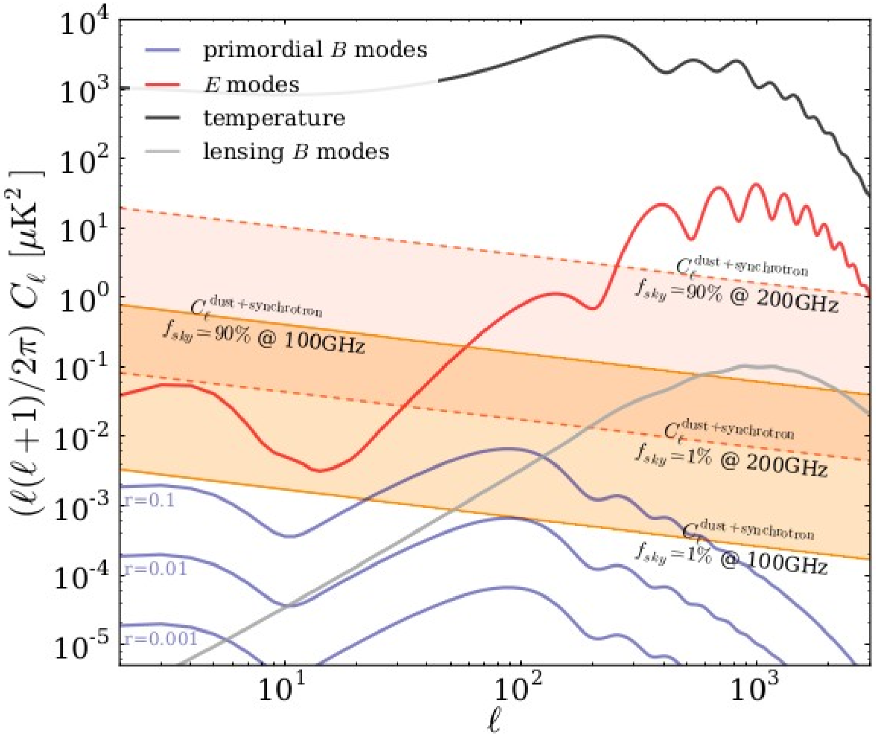

Errard et al, 2015

Highly polarized Galactic foregrounds

@ any frequency
@ any direction on the sky
@ any angular scale

many orders of magnitude larger than primordial CMB B-modes

- Spectral information on polarized foregrounds is non-trivial
  - *synchrotron curvature ?*
  - *how many greybodies for thermal dust ?*

- How many polarized foregrounds in the sky ?
  - *thermal dust*
  - *synchrotron*
  - *spinning dust ?*
  - *magnetic dust ?*
  - *polarized CO ?*
  - *… ?*

the answer not only depends on physics but also on instrument sensitivity

Bayesian parametric fitting & Gibbs sampling

COMMANDER - *Eriksen et al (2008)*

Parametric fitting model

$$
\begin{aligned}
\boldsymbol{m}(p,\nu) &= a(\nu)\,\boldsymbol{s}^{cmb}(p) \\
&+ \left(\frac{\nu}{\nu_0^s}\right)^{\beta_s(p)} \boldsymbol{s}^{sync}(p) \\
&+ \left(\frac{\nu}{\nu_0^d}\right)^{\beta_d(p)} B_\nu\left(T_d(p)\right)\boldsymbol{s}^{dust}(p) \\
&+ \boldsymbol{n}(p,\nu)
\end{aligned}
$$

MCMC Gibbs sampling

- amplitudes (CMB, dust, synchrotron) $\boldsymbol{s}^{(i+1)} \leftarrow P\left(\boldsymbol{s}\middle|C_\ell^{(i)},\boldsymbol{\beta}^{(i)},\boldsymbol{d}\right)$
- CMB power spectra $C_\ell^{(i+1)} \leftarrow P\left(C_\ell\middle|\boldsymbol{s}^{(i+1)}\right)$
- Foreground spectral indices $\boldsymbol{\beta}^{(i+1)} \leftarrow P\left(\boldsymbol{\beta}\middle|\boldsymbol{s}^{(i+1)},\boldsymbol{d}\right)$

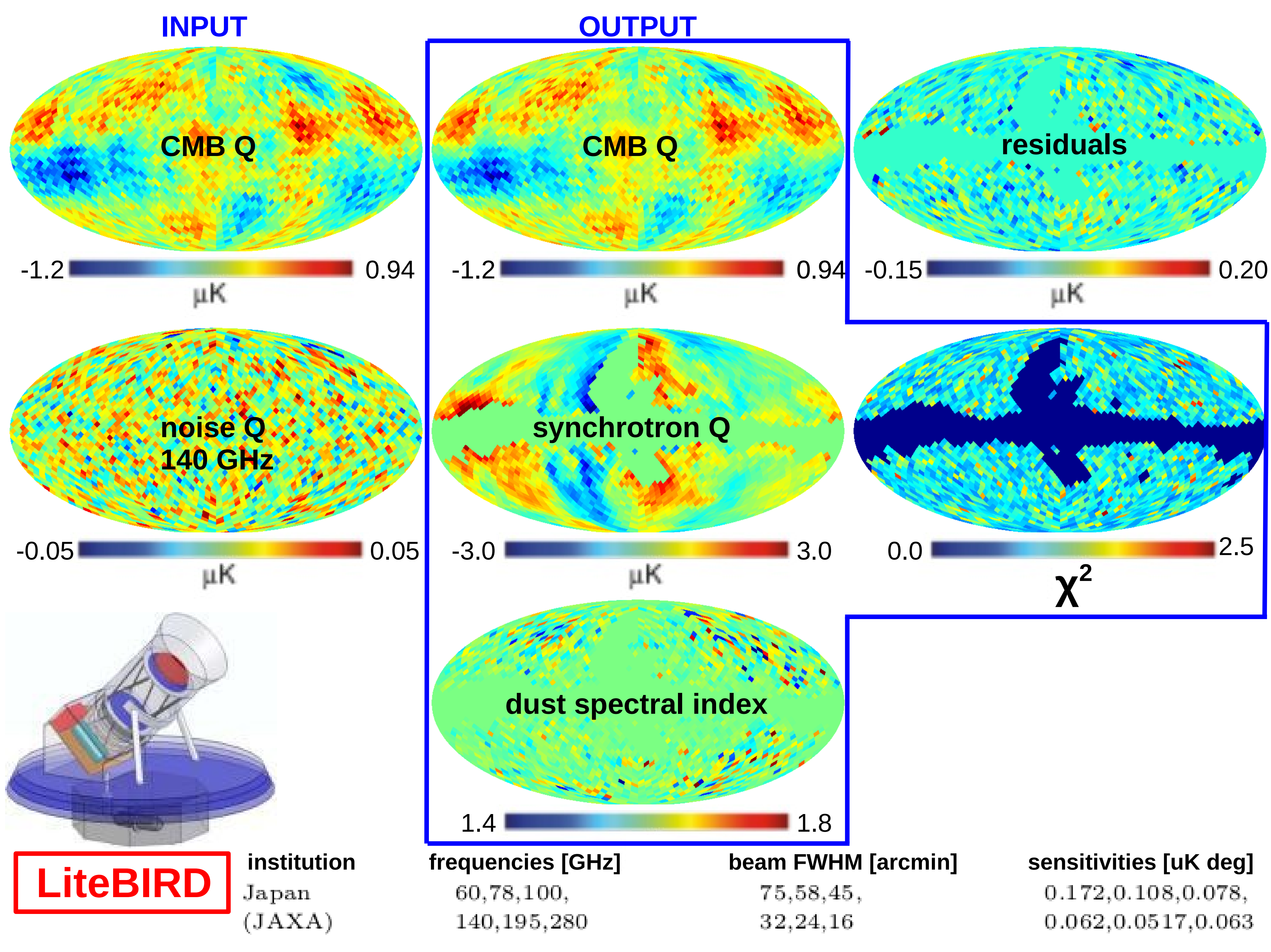

INPUT
OUTPUT
CMB Q
-1.2
0.94
μK
CMB Q
-1.2
0.94
μK
residuals
-0.15
0.20
μK
noise Q
140 GHz
-0.05
0.05
μK
synchrotron Q
-3.0
3.0
μK
0.0
2.5
χ2
dust spectral index
1.4
1.8
LiteBIRD
institution
Japan
(JAXA)
frequencies [GHz]
60,78,100,
140,195,280
beam FWHM [arcmin]
75,58,45,
32,24,16
sensitivities [uK deg]
0.172,0.108,0.078,
0.062,0.0517,0.063

Likelihood distribution of the tensor-to-scalar

After foreground removal :

$C^{EE}_{\ell<12} \propto \tau^2$ (optical depth to reionization)

$C^{BB}_{\ell<12} \propto r$ (tensor-to-scalar ratio)

$$\mathcal{L}\left(C_\ell \middle| \tau, r\right) \propto \frac{e^{-\frac{1}{2}\left[C_\ell - C_\ell^{th}(\tau,r)\right]\Sigma^{-1}\left[C_\ell - C_\ell^{th}(\tau,r)\right]}}{\Sigma^{1/2}}$$

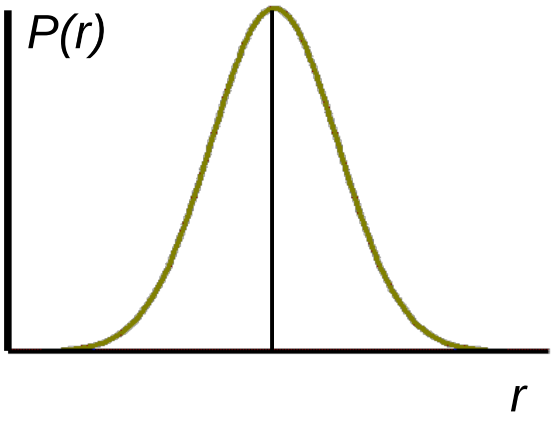

Impact of incorrect foreground modelling ?

possible mismatch between the foreground model and the data

$$
\begin{aligned}
\boldsymbol{m}(p,\nu) &= a(\nu)\,\boldsymbol{s}^{cmb}(p) \\
&+ \left(\frac{\nu}{\nu_0^s}\right)^{\beta_s(p)} \boldsymbol{s}^{sync}(p) \\
&+ \left(\frac{\nu}{\nu_0^d}\right)^{\beta_d(p)} B_\nu\left(T_d(p)\right)\boldsymbol{s}^{dust}(p) \\
&+ \boldsymbol{n}(p,\nu)
\end{aligned}
$$

Model

$$
\begin{aligned}
\boldsymbol{d}(p,\nu) &= a(\nu)\,\boldsymbol{s}^{cmb}(p) \\
&+ \left(\frac{\nu}{\nu_0^s}\right)^{\beta_s(p) + C\ln(\nu/\nu_0^s)} \boldsymbol{s}^{sync}(p) \\
&+ \left[f_1\left(\frac{\nu}{\nu_0^d}\right)^{\beta_1(p)} B_\nu\left(T_1(p)\right) + f_2\left(\frac{\nu}{\nu_0^d}\right)^{\beta_2(p)} B_\nu\left(T_2(p)\right)\right]\boldsymbol{s}^{dust}(p) \\
&+ \epsilon(\nu)\,\boldsymbol{s}^{spinning\ dust}(p) \\
&+ \boldsymbol{n}(p,\nu)
\end{aligned}
$$

synchrotron curvature

extra thermal dust

spinning dust

Data

Remazeilles, Dickinson, Eriksen, Wehus, *arXiv:1509.04714*

Correct foreground modelling

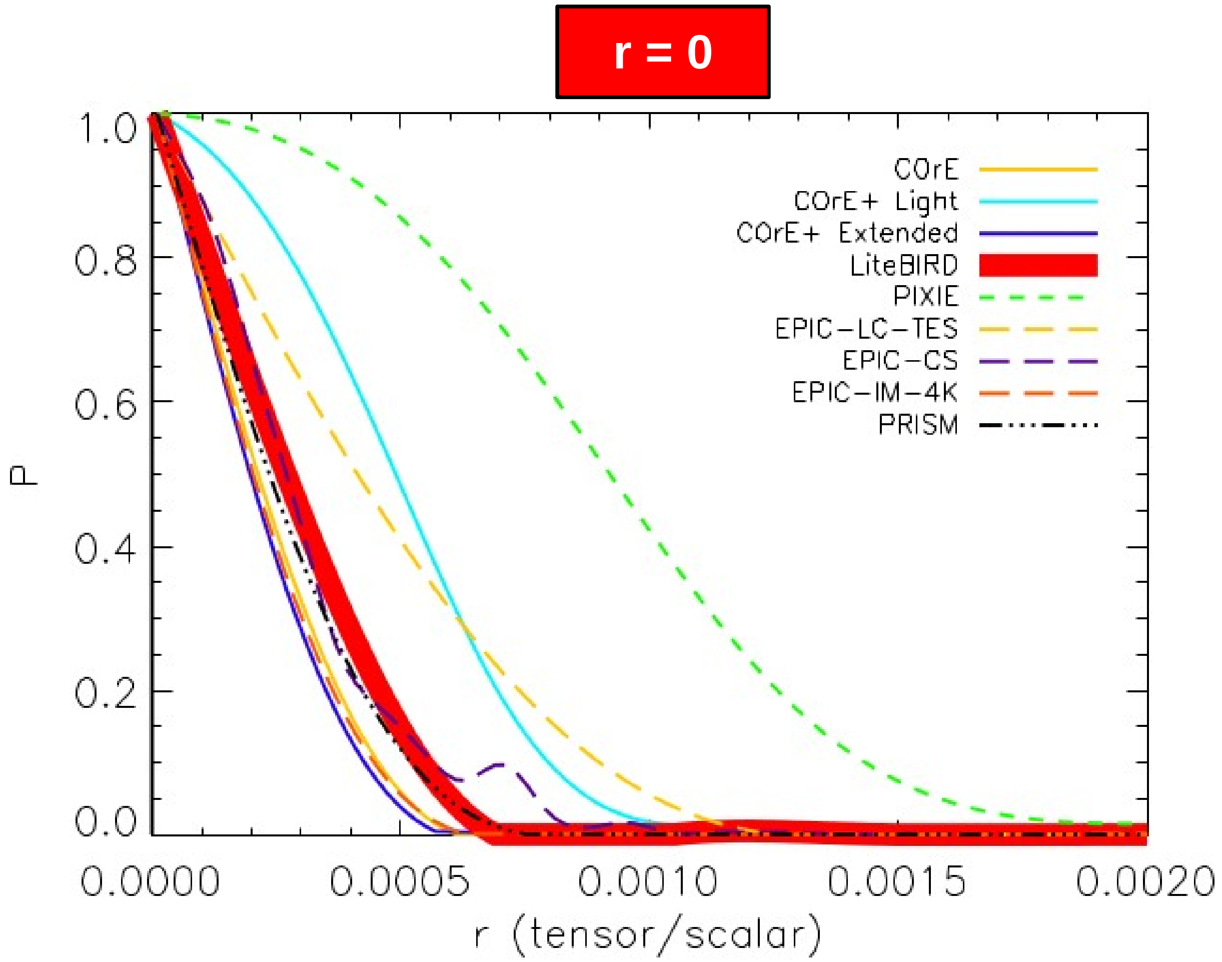

LiteBIRD

Remazeilles, Dickinson, Eriksen, Wehus, *arXiv:1509.04714*

Correct foreground modelling

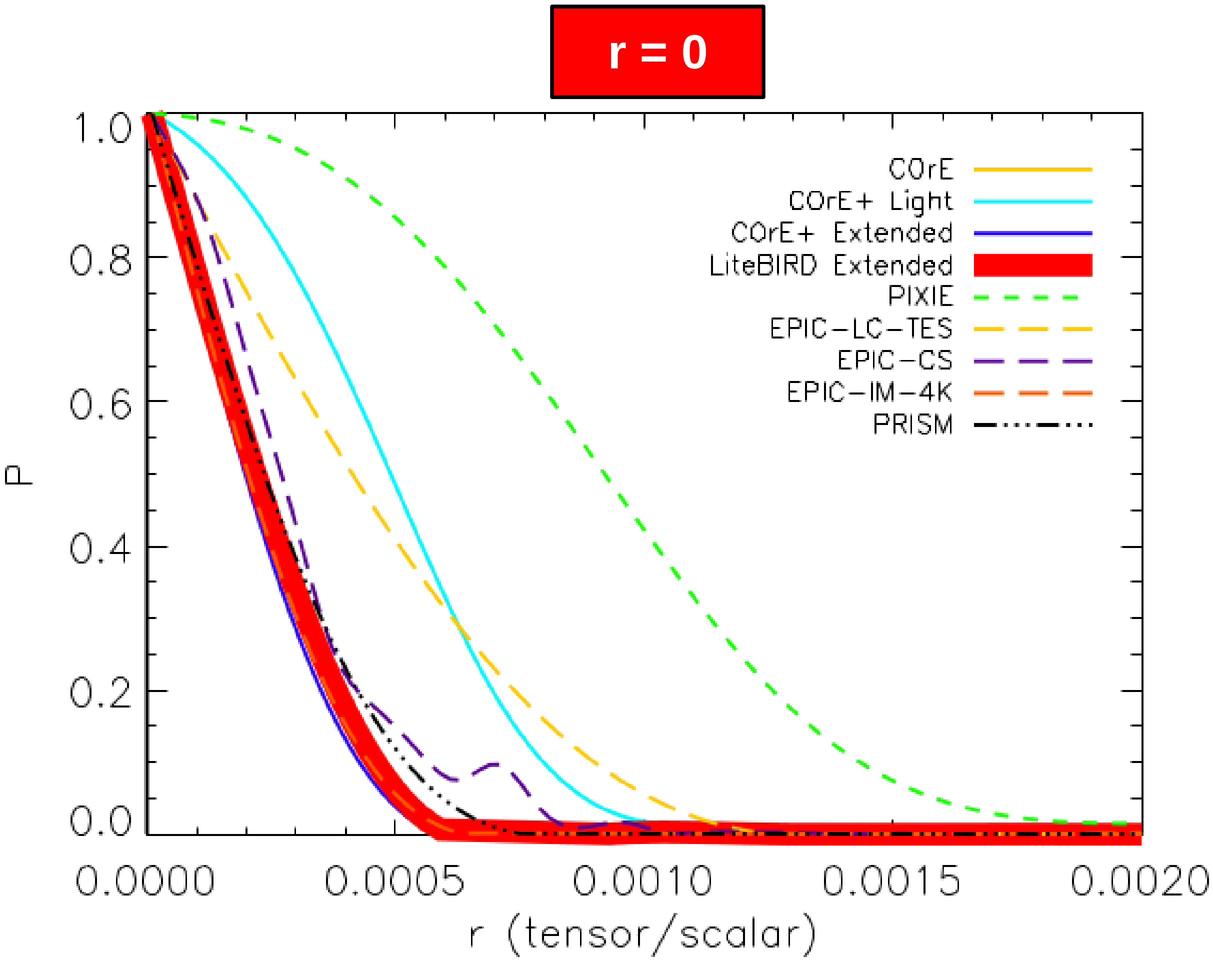

LiteBIRD extended

*Extra low-frequency channels help in reducing the uncertainty on **r***

Remazeilles, Dickinson, Eriksen, Wehus, *arXiv:1509.04714*

No foreground: overall sensitivity

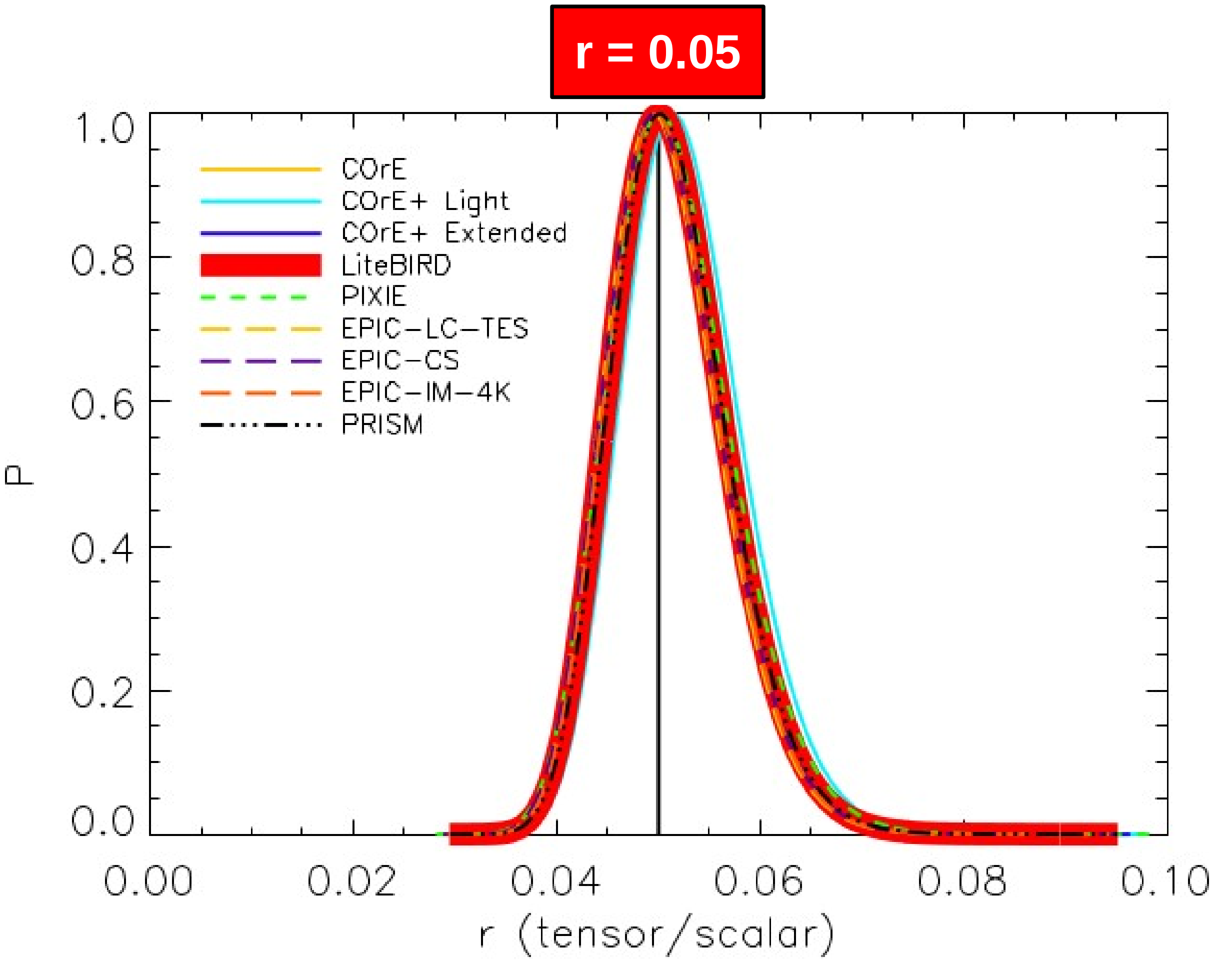

*errors on **r** dominated by cosmic variance for all satellite concepts*

$\ell_{max} \sim 12$

χ^2	r	
0.99	0.05271 ± 0.00595	COrE+ Light
0.99	0.05202 ± 0.00585	COrE+ Extended
0.98	0.05107 ± 0.00575	COrE
0.96	0.05132 ± 0.00578	LiteBIRD
0.99	0.05145 ± 0.00616	PIXIE
0.97	0.05074 ± 0.00572	EPIC-LC-TES
0.96	0.05086 ± 0.00583	EPIC-CS
0.97	0.05096 ± 0.00572	EPIC-IM-4K
0.99	0.05140 ± 0.00578	PRISM

9σ detection

Remazeilles, Dickinson, Eriksen, Wehus, *arXiv:1509.04714*

Correct foreground modelling

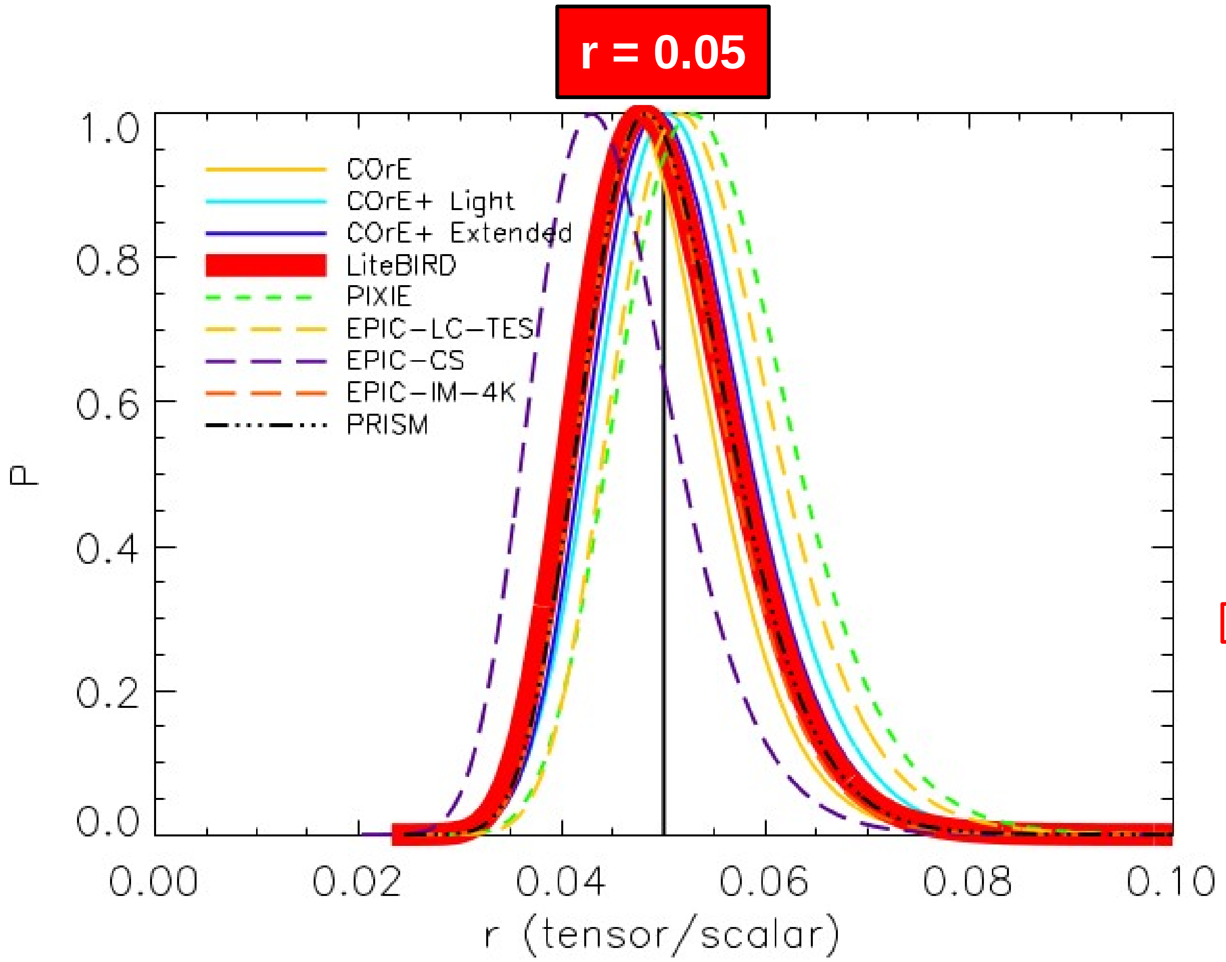

Galactic foregrounds inflate the error on ***r*** *but there is no bias*

$\ell_{max} \sim 12$

χ^2	*r*	
1.00	0.05224 ± 0.00800	COrE+ Light
0.99	0.05132 ± 0.00770	COrE+ Extended
0.99	0.04877 ± 0.00715	COrE
0.99	0.04997 ± 0.00767	LiteBIRD
1.00	0.05507 ± 0.00865	PIXIE
1.06	0.05411 ± 0.00823	EPIC-LC-TES
0.97	0.04506 ± 0.00730	EPIC-CS
0.98	0.04989 ± 0.00708	EPIC-IM-4K
1.00	0.05027 ± 0.00737	PRISM

6.5σ detection

Remazeilles, Dickinson, Eriksen, Wehus, *arXiv:1509.04714*

Incorrect dust modelling : omitting one greybody component

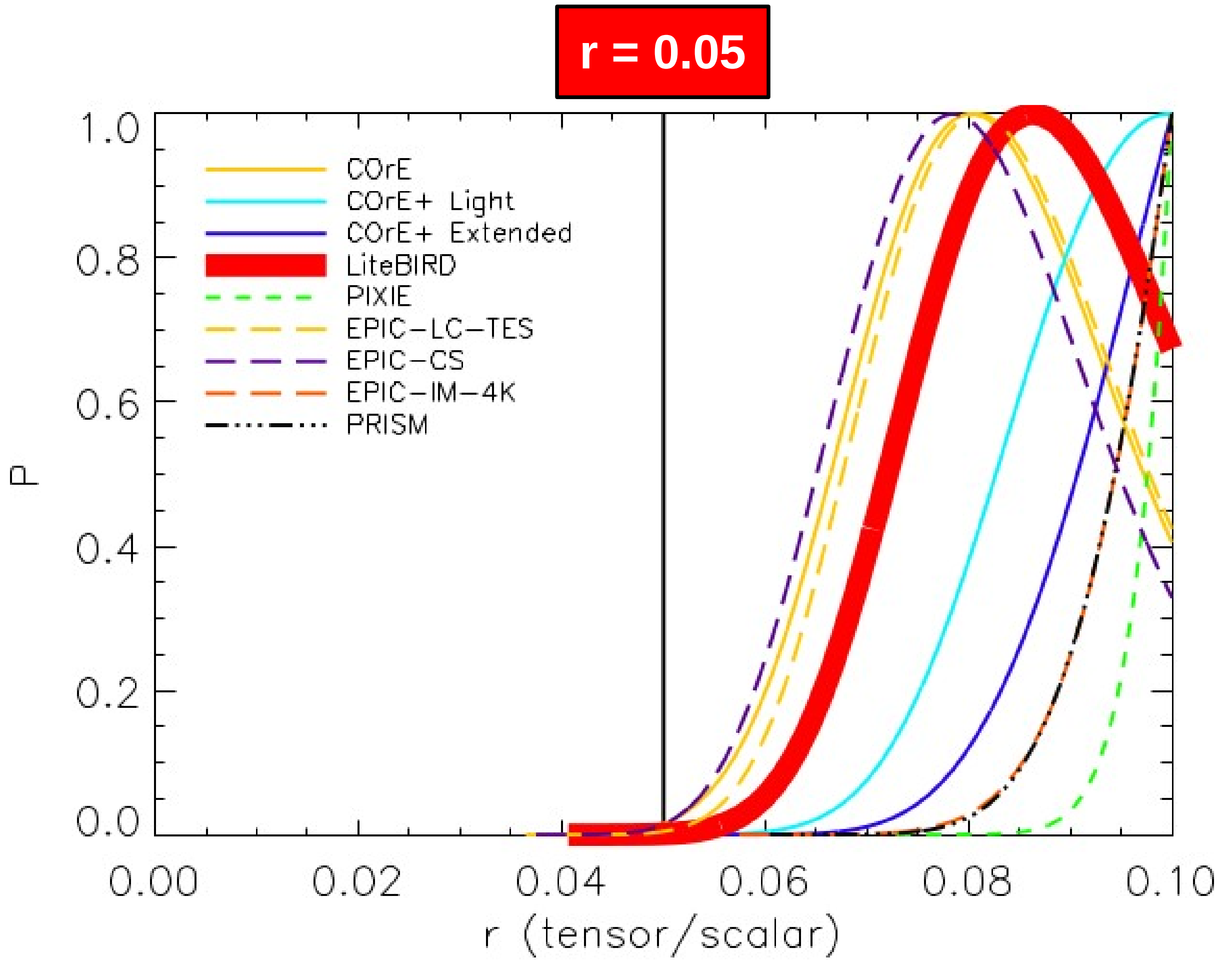

Incorrect spectral modelling of thermal dust strongly bias the most sensitive experiments

$\ell_{max} \sim 12$

χ^2	r	
1.07	0.08929 ± 0.00766	COrE+ Light
1.20	0.09218 ± 0.00624	COrE+ Extended
1.12	0.08023 ± 0.01045	COrE
1.10	0.08428 ± 0.00935	LiteBIRD
1.08	0.09711 ± 0.00265	PIXIE
1.32	0.08113 ± 0.00999	EPIC-LC-TES
1.08	0.07911 ± 0.01048	EPIC-CS
2.88	0.09434 ± 0.00485	EPIC-IM-4K
1.58	0.09446 ± 0.00467	PRISM

4σ bias

Remazeilles, Dickinson, Eriksen, Wehus, *arXiv:1509.04714*

Incorrect synchrotron modelling : neglecting curvature

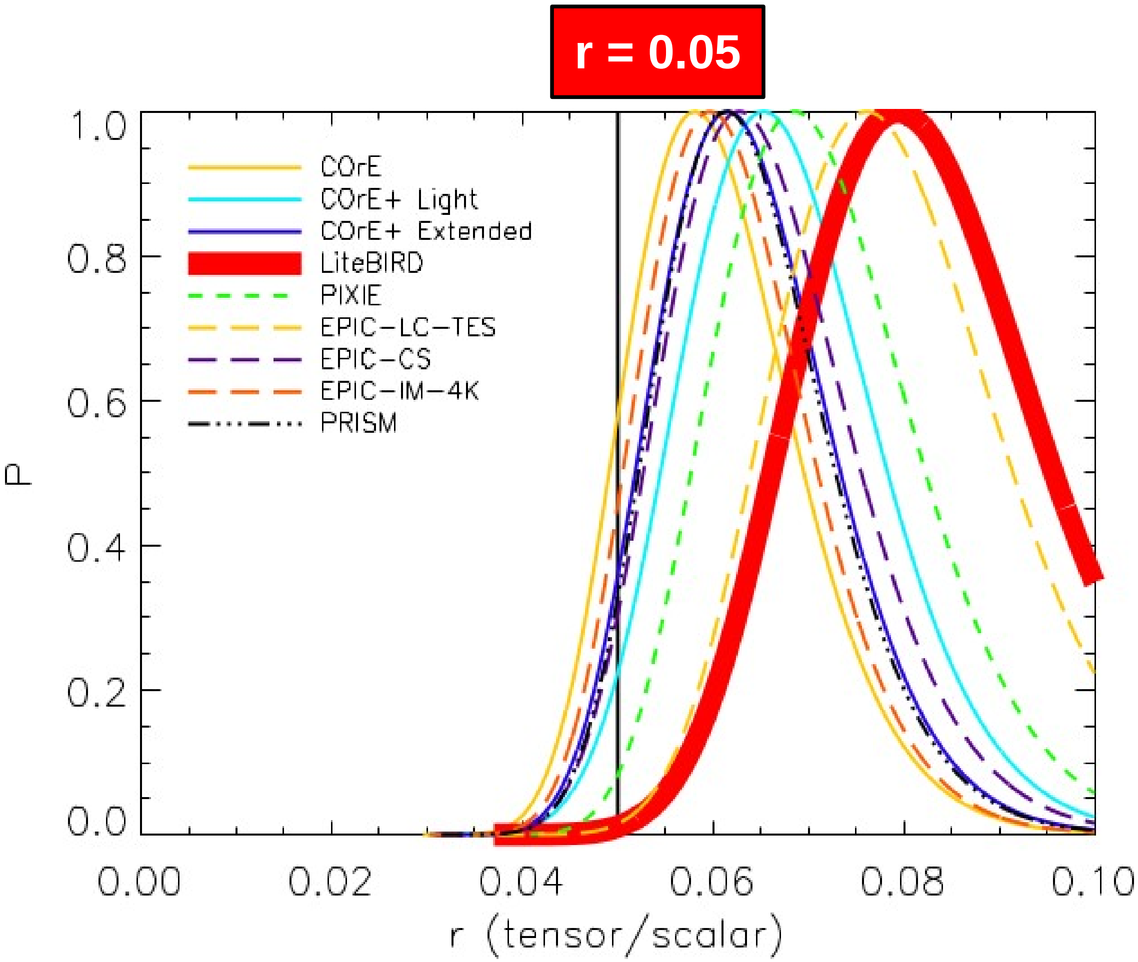

Incorrect spectral modelling of synchrotron bias the tensor-to-scalar ratio by > 1σ

$\ell_{max} \sim 12$

χ^2	*r*	
1.00	0.06756 ± 0.01027	COrE+ Light
1.01	0.06390 ± 0.00946	COrE+ Extended
1.01	0.06074 ± 0.00920	COrE
1.01	0.07988 ± 0.01027	LiteBIRD
1.01	0.07122 ± 0.01027	PIXIE
1.09	0.07769 ± 0.01029	EPIC-LC-TES
0.99	0.06558 ± 0.01004	EPIC-CS
1.30	0.06205 ± 0.00906	EPIC-IM-4K
1.12	0.06386 ± 0.00925	PRISM

low χ^2 but large bias on *r*

→ lack of channels to fit non-trivial synchrotron

LiteBIRD

Remazeilles, Dickinson, Eriksen, Wehus, *arXiv:1509.04714*

Curvature flattens the synchrotron spectrum

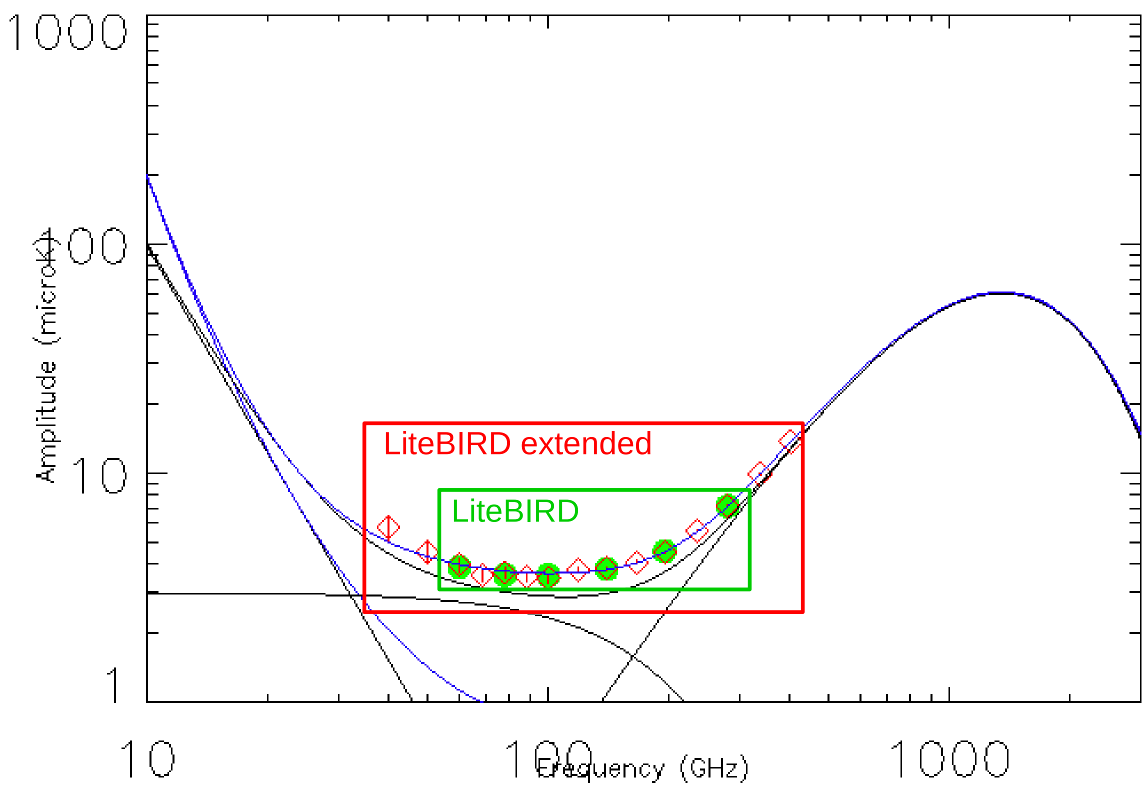

Curvature makes synchrotron and CMB components less “orthogonal”

- Over the frequency range of **LiteBIRD**, curvature prevents any component separation method (COMMANDER, NILC) from distinguishing between the CMB spectrum and the synchrotron spectrum flattened by curvature
- → the fit of the total sky will be correct (χ^2~1) but the synchrotron and the CMB will not be correctly separated
- **LiteBIRD extended** can distinguish between synchrotron curvature and CMB through extra low-frequency channels (< 60 GHz)

Incorrect synchrotron modelling : neglecting curvature

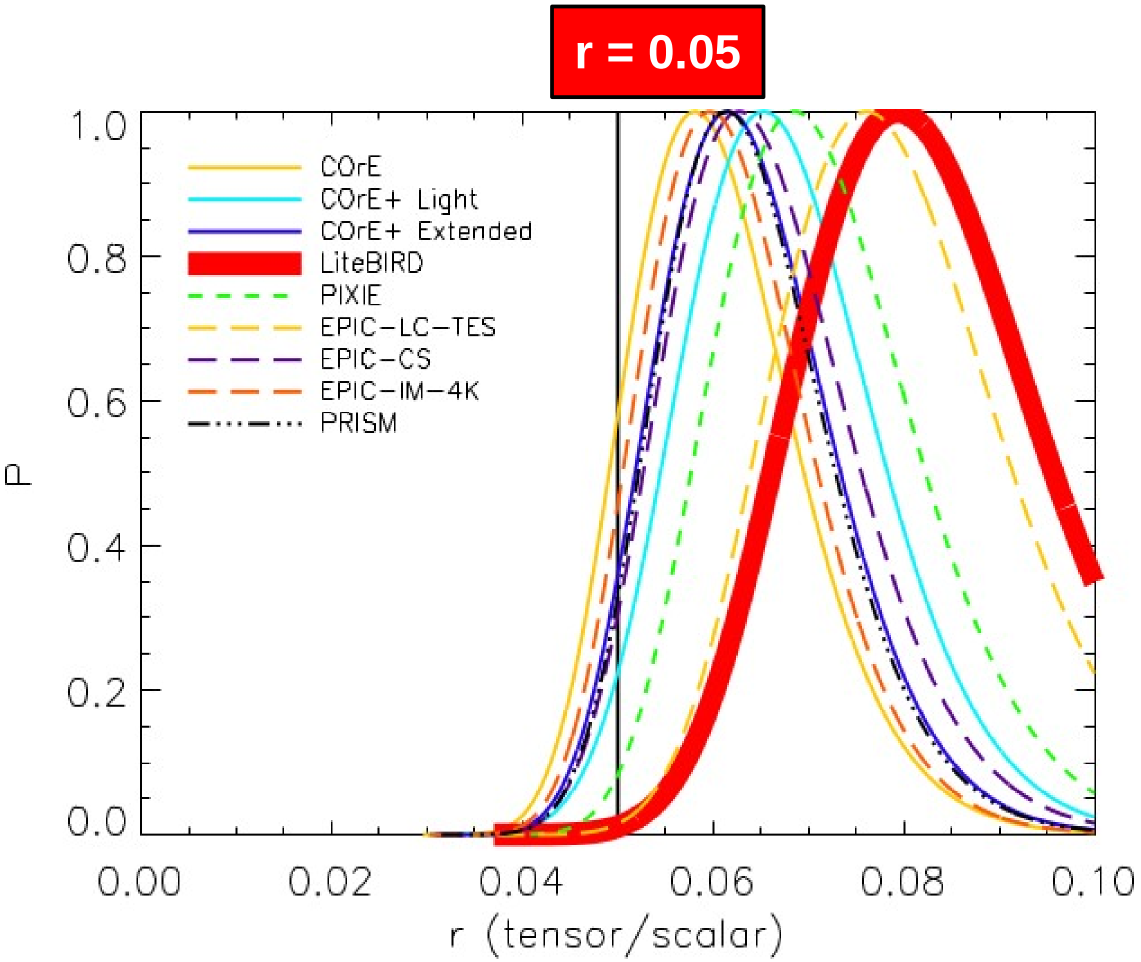

Incorrect spectral modelling of synchrotron bias the tensor-to-scalar ratio by > 1σ

$\ell_{max} \sim 12$

LiteBIRD

Remazeilles, Dickinson, Eriksen, Wehus, *arXiv:1509.04714*

Incorrect synchrotron modelling : neglecting curvature

r = 0.05

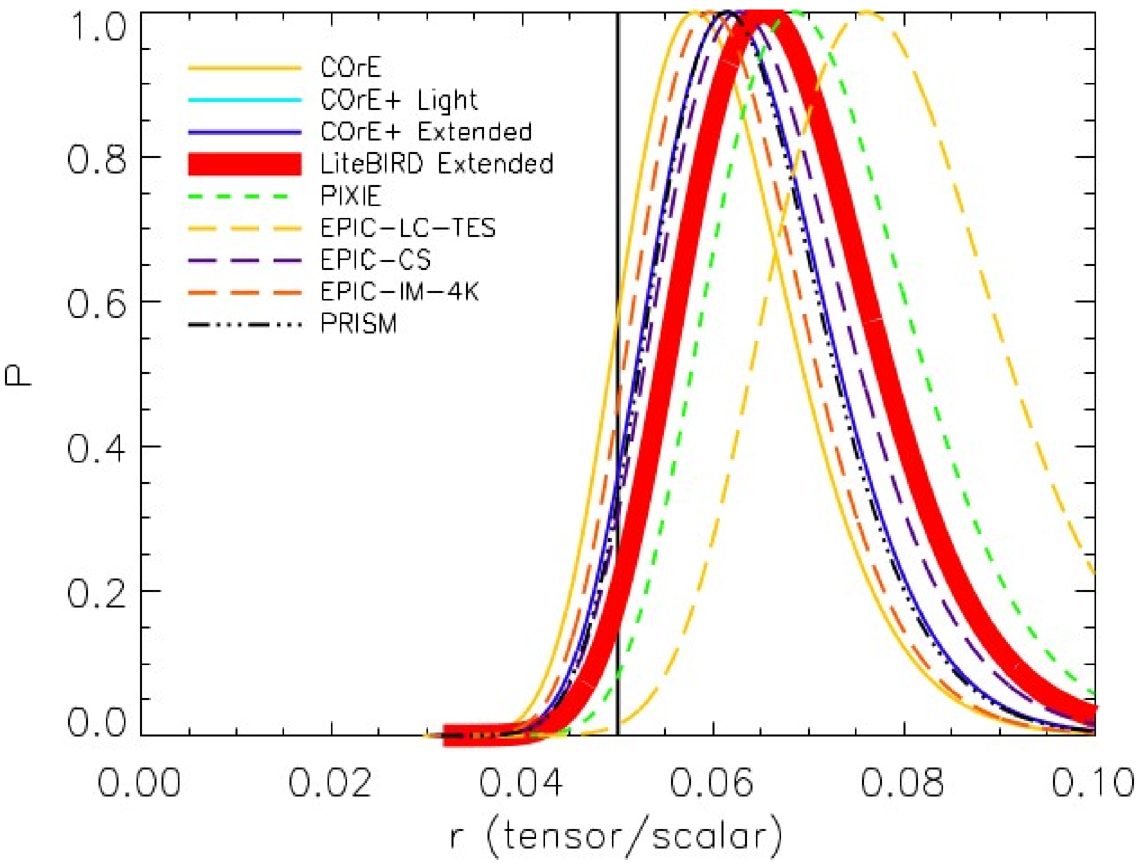

Incorrect spectral modelling of synchrotron bias the tensor-to-scalar ratio by > 1σ

$\ell_{max} \sim 12$

LiteBIRD extended

Remazeilles, Dickinson, Eriksen, Wehus, *arXiv:1509.04714*

Summary

- Full Bayesian framework: sky component fitting & likelihood estimation of ***r***
  - End-to-end propagation of foreground uncertainties to cosmological parameters
    → next step: systematics and lensing uncertainties
  - Feedback on foreground modelling through the χ^2 output map
- 2 criteria : χ^2 statistics of the fit & tensor-to-scalar ratio ***r***
  - Taken together, they indicate wether a false detection of ***r*** is due to incorrect foreground modelling or lack of low frequency channels
- Because of unprecedented sensitivity, next-generation CMB satellites are much more sensitive to incorrect assumptions about Galactic foregrounds
  - Omitting one extra greybody dust component → ***r*** biased by more than 3σ
  - Neglecting synchrotron curvature (C=0.3) → ***r*** biased by more than 1σ
  - Neglecting 1% spinning dust polarization → ***r*** non-negligible bias
- "LiteBIRD extended" better controls foreground uncertainties than "LiteBIRD original"
  - LiteBIRD extended can distinguish between CMB and synchrotron curvature through extra-low frequency channels

Backup slides

LiteBIRD extended

Frequencies (GHz)

40
50
60
68.4
78.0
88.5
100.0
118.9
140.0
166.0
195
234.9
280
337.4
402.1

Missing polarized foreground : spinning dust

0.00049 ± 0.00028
0.00019 ± 0.00014
0.00057 ± 0.00041
0.00029 ± 0.00025
0.00076 ± 0.00050
0.00647 ± 0.00135
0.00173 ± 0.00058
0.00029 ± 0.00023
0.00036 ± 0.00028

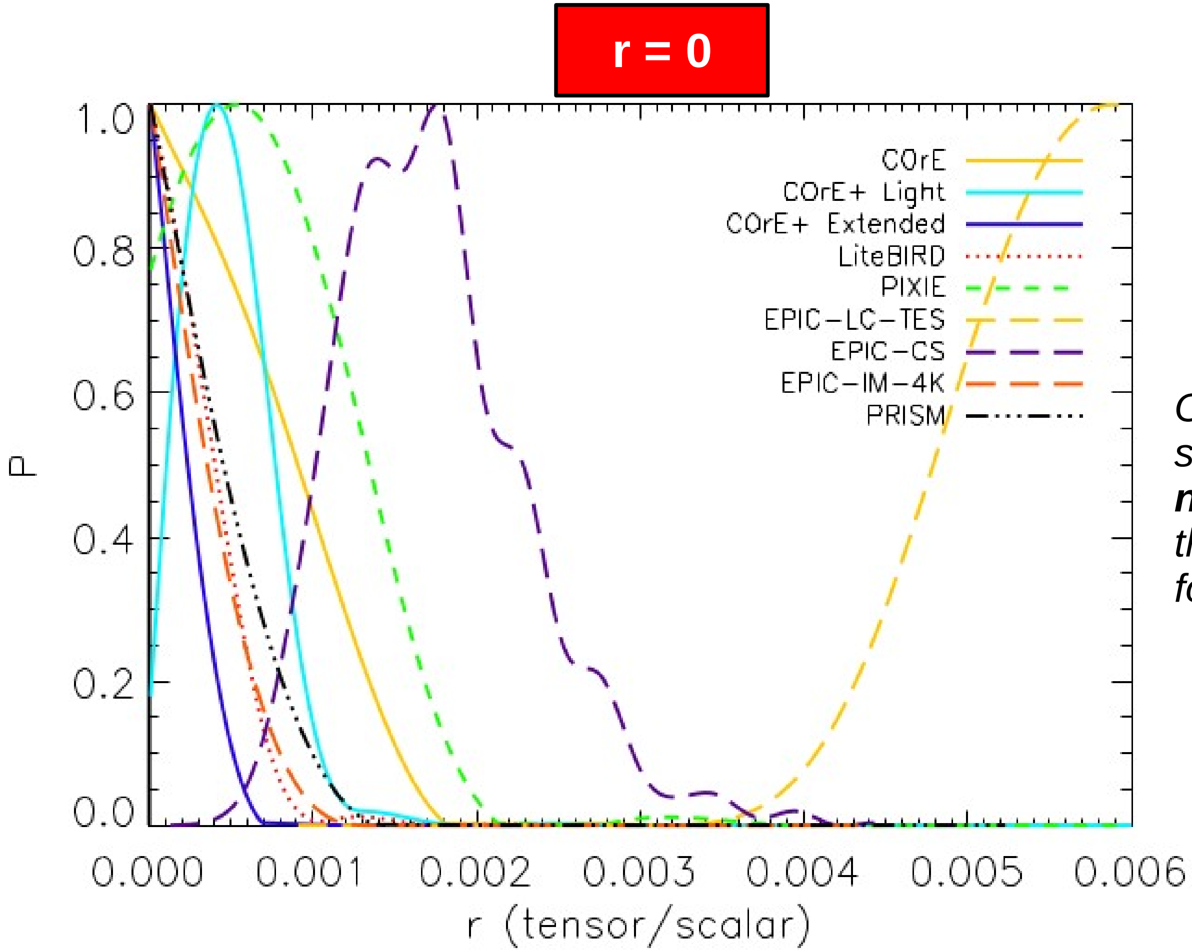

Omitting the 1% polarized spinning dust makes a ***non-negligible bias*** *on the tensor-to-scalar ratio for some experiments*

$\ell_{max} \sim 12$

Remazeilles, Dickinson, Eriksen, Wehus, *in prep. (2015)*

Correct foreground modelling

r = 0

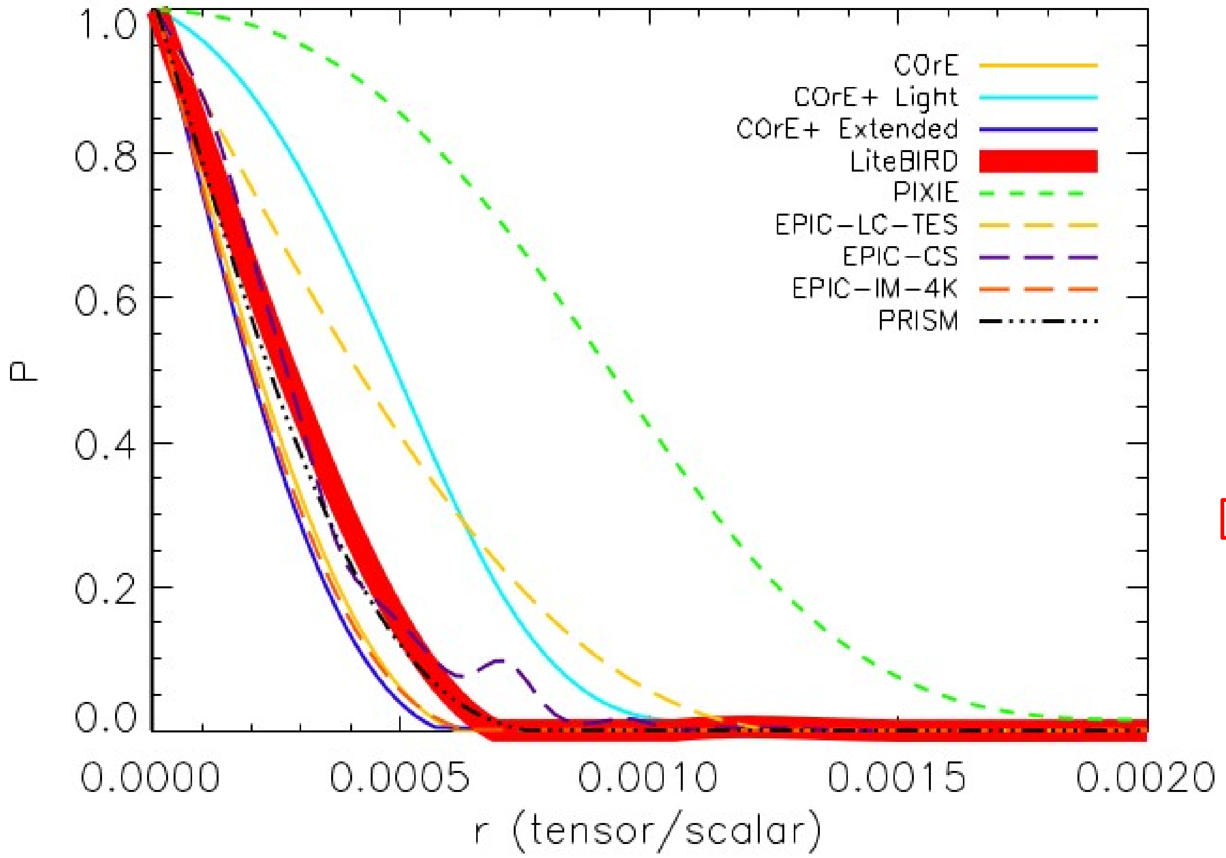

Galactic foregrounds inflate the error on ***r*** *but there is no bias*

$\ell_{max} \sim 12$

χ^2	r	
1.00	0.00031 ± 0.00024	COrE+ Light
0.99	0.00016 ± 0.00012	COrE+ Extended
0.99	0.00017 ± 0.00013	COrE
0.99	0.00020 ± 0.00017	LiteBIRD
0.99	0.00056 ± 0.00042	PIXIE
1.06	0.00033 ± 0.00026	EPIC-LC-TES
0.97	0.00023 ± 0.00020	EPIC-CS
0.98	0.00016 ± 0.00013	EPIC-IM-4K
0.99	0.00019 ± 0.00015	PRISM

Remazeilles, Dickinson, Eriksen, Wehus, *arXiv:1509.04714*

Incorrect dust modelling : omitting one greybody component

r = 0

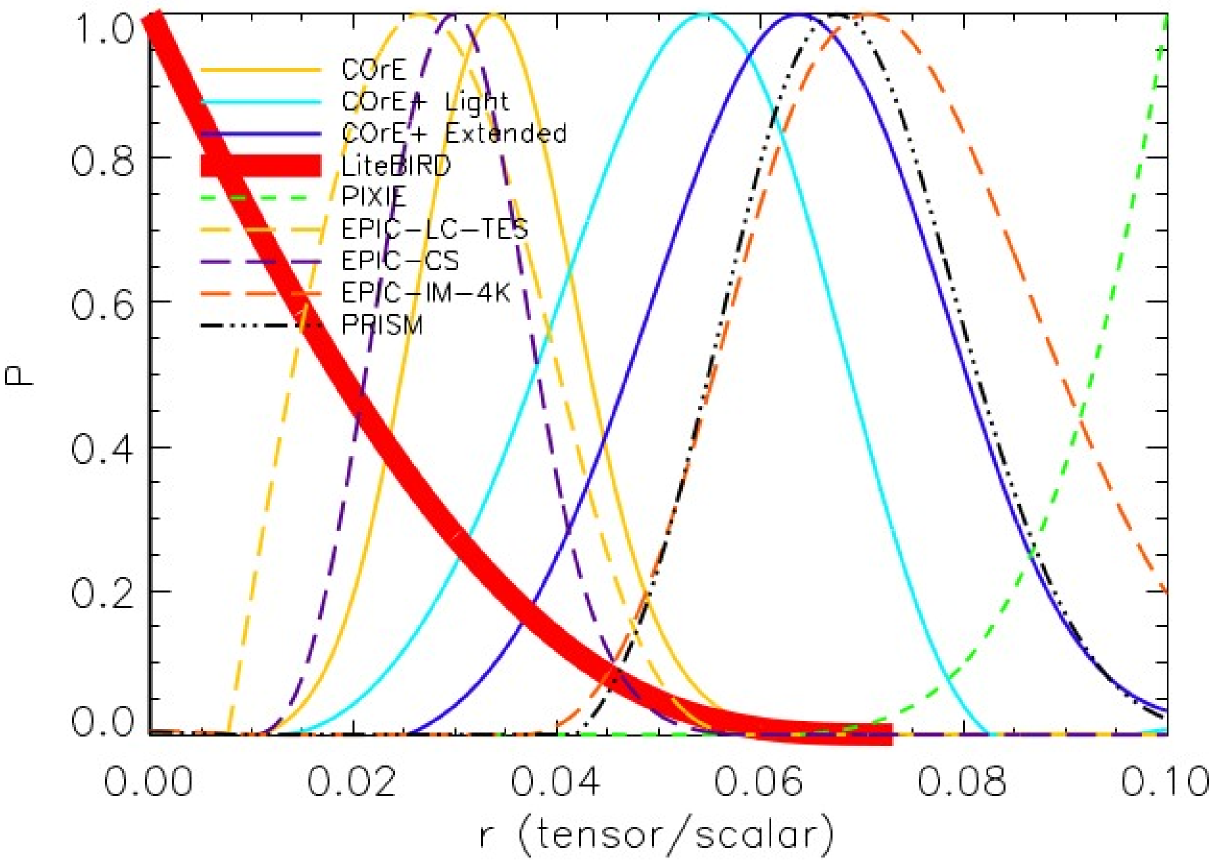

Incorrect spectral modelling of thermal dust strongly bias the most sensitive experiments

$\ell_{max} \sim 12$

χ^2	r	
1.07	0.05229 ± 0.01223	COrE+ Light
1.20	0.06357 ± 0.01332	COrE+ Extended
1.12	0.03453 ± 0.00821	COrE
1.10	0.01595 ± 0.01249	LiteBIRD
1.08	0.09246 ± 0.00635	PIXIE
1.33	0.02792 ± 0.00936	EPIC-LC-TES
1.08	0.03018 ± 0.00699	EPIC-CS
2.88	0.07251 ± 0.01265	EPIC-IM-4K
1.58	0.06885 ± 0.01068	PRISM

High-frequency channels very useful to highlight failure in dust model

Remazeilles, Dickinson, Eriksen, Wehus, *arXiv:1509.04714*

Incorrect foreground modelling : minor impact on Planck

Armitage-Caplan et al., *MNRAS 2012*

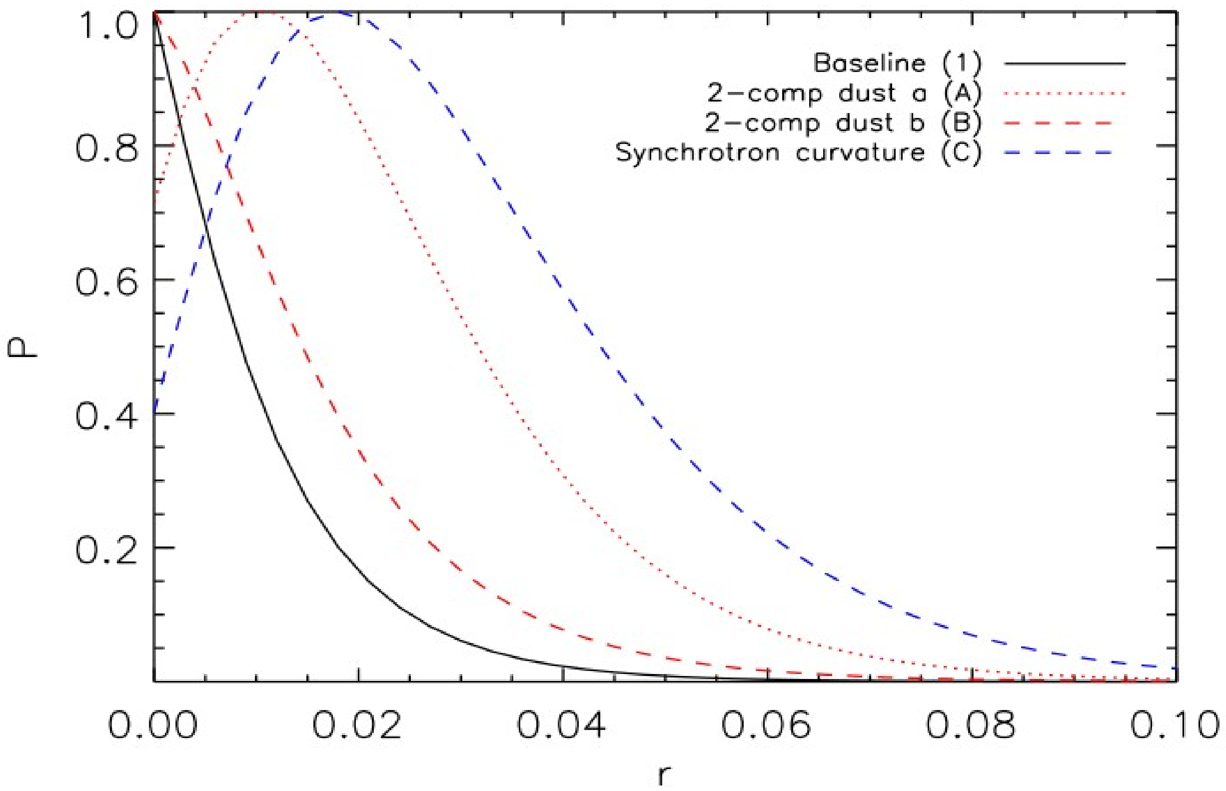

$\ell_{max} \sim 12$

- *Because of lower sensitivity, <u>Planck is less impacted</u> by incorrect spectral assumptions on the Galactic foregrounds*

Incorrect dust modelling : impact of high frequency channels

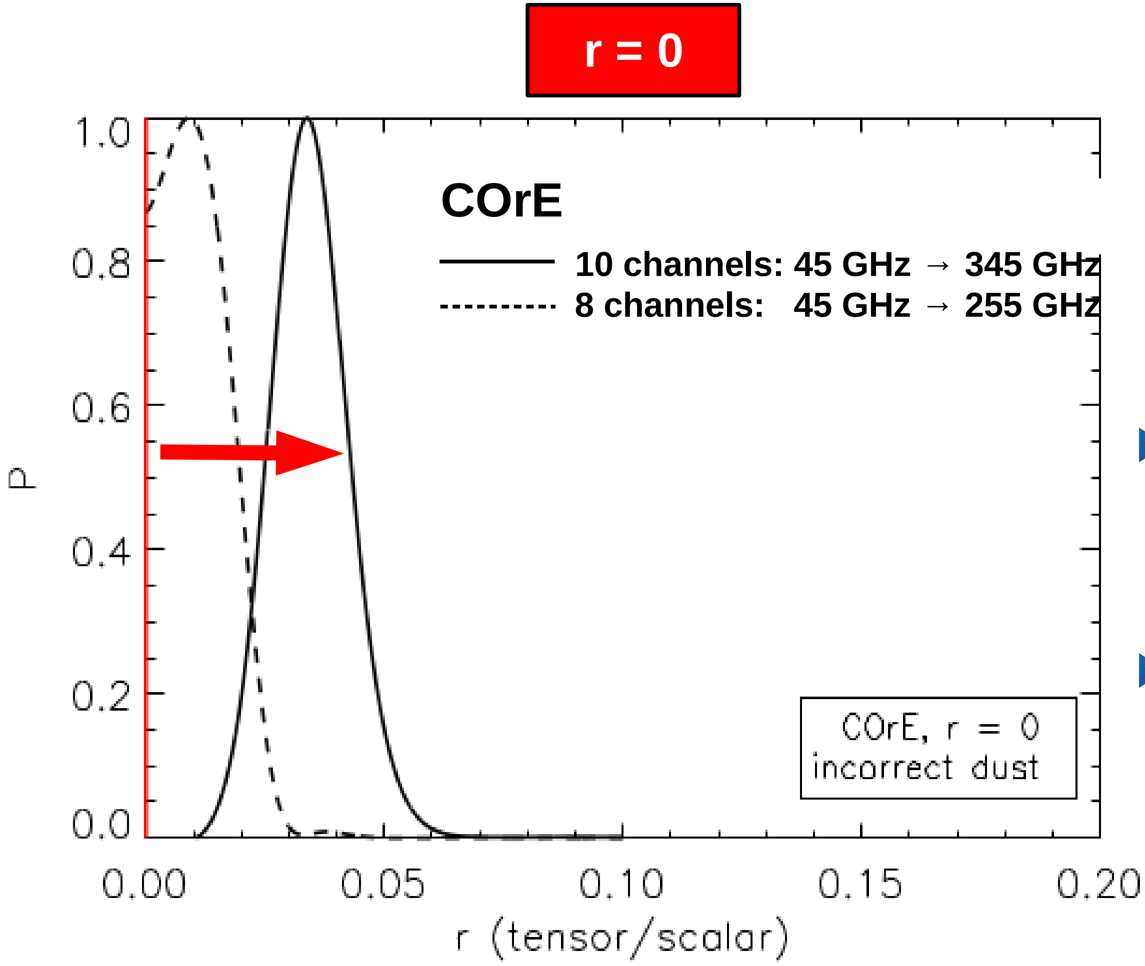

- ***High-frequency channels useful to highlight any failure in the model of polarized dust***
- *Instability of P(r) distribution with respect to frequencies highlights spurious detection of dust B-modes*

Remazeilles, Dickinson, Eriksen, Wehus, *arXiv:1509.04714*

Incorrect dust modelling : impact of Galactic masking

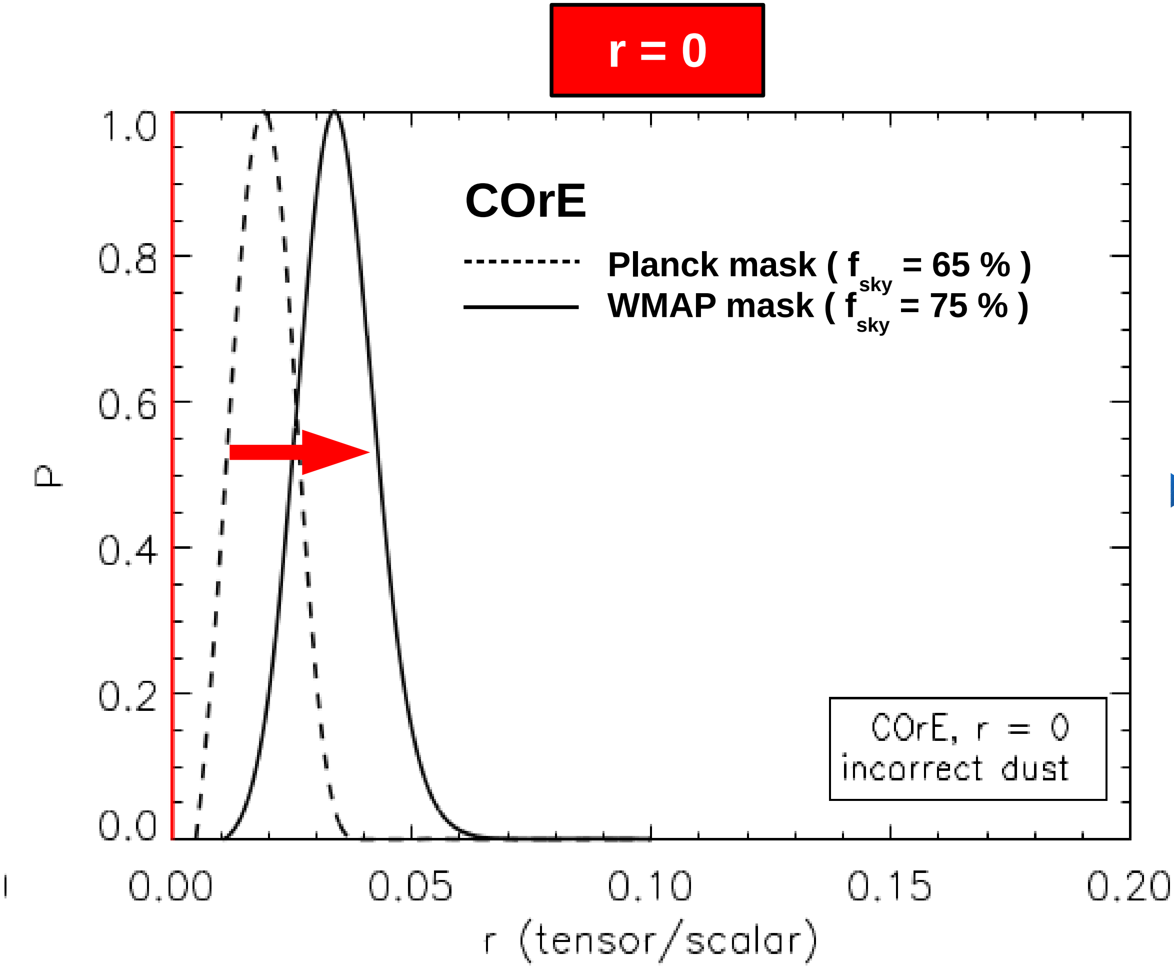

- *Instability of P(r) distribution with respect to the size of the mask highlights spurious detection of dust B-modes*

Remazeilles, Dickinson, Eriksen, Wehus, *arXiv:1509.04714*

MCMC Gibbs sampling

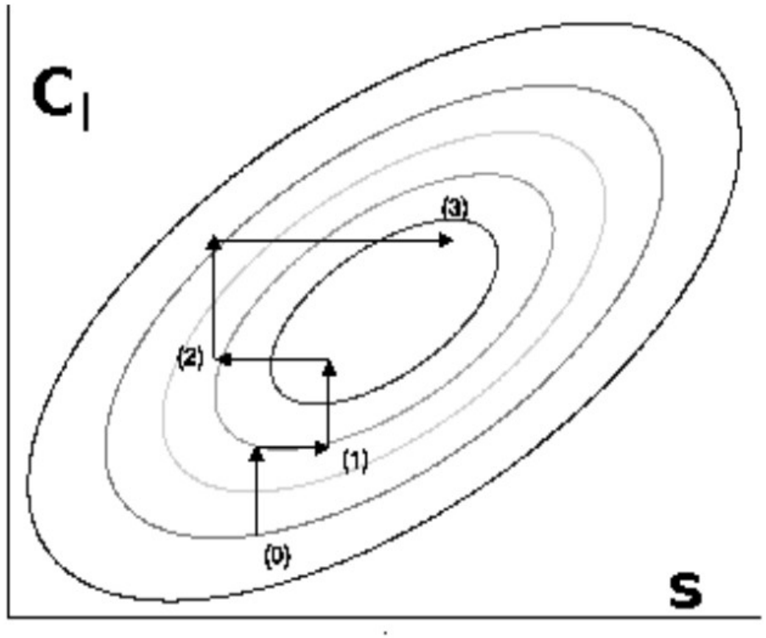

$$\boldsymbol{s}^{(i+1)} \leftarrow P\left(\boldsymbol{s} \middle| C_\ell^{(i)}, \boldsymbol{d}\right)$$

$$C_\ell^{(i+1)} \leftarrow P\left(C_\ell \middle| \boldsymbol{s}^{(i+1)}, \boldsymbol{d}\right)$$

C_ℓ sampling

$$P\left(C_\ell \middle| \boldsymbol{s}, \boldsymbol{d}\right) = P\left(C_\ell \middle| \boldsymbol{s}\right) \propto \frac{e^{-\frac{(2\ell+1)}{2C_\ell}\left(\frac{1}{2l+1}\sum_{m=-\ell}^{\ell} |\boldsymbol{s}_{\ell m}|^2\right)}}{C_\ell^{(2\ell+1)/2}}$$

- Inverse-Gamma distribution
- Simple textbook sampling algorithm $\rightarrow C_\ell^{(i+1)}$

Amplitude sampling

$$P\left(\boldsymbol{s}\middle|C_\ell, \boldsymbol{d}\right) \propto P\left(\boldsymbol{d}\middle|\boldsymbol{s}, C_\ell\right) P\left(\boldsymbol{s}\middle|C_\ell\right)$$
$$\propto e^{(-1/2)(\boldsymbol{d}-\boldsymbol{s})^T \boldsymbol{N}^{-1}(\boldsymbol{d}-\boldsymbol{s})} e^{(-1/2)\boldsymbol{s}^T \boldsymbol{S}^{-1}\boldsymbol{s}}$$
$$\propto e^{(-1/2)(\boldsymbol{s}-\widehat{\boldsymbol{s}})^T \left(\boldsymbol{S}^{-1}+\boldsymbol{N}^{-1}\right)(\boldsymbol{s}-\widehat{\boldsymbol{s}})}$$

- Gaussian distribution where $\widehat{\boldsymbol{s}} = \left(\boldsymbol{S}^{-1} + \boldsymbol{N}^{-1}\right)^{-1} \boldsymbol{N}^{-1}\boldsymbol{d}$ is the Wiener
- $\boldsymbol{s}^{(i+1)}$ is solution (conjugate gradients) of

$$\left(\boldsymbol{S}^{-1} + \boldsymbol{N}^{-1}\right)\boldsymbol{s} = \boldsymbol{N}^{-1}\boldsymbol{d} + \boldsymbol{S}^{-1/2} w_0 + \boldsymbol{N}^{-1/2} w_1$$

where $w_0, w_1 \sim \mathcal{N}(0, 1)$